


## Article

# Insight into the Degradation of Two Benzophenone-Type UV Filters by the UV/H<sub>2</sub>O<sub>2</sub> Advanced Oxidation Process

Erdeng Du <sup>1</sup>, Jiaqi Li <sup>1</sup>, Siqi Zhou <sup>1</sup>, Miao Li <sup>2,\*</sup>, Xiang Liu <sup>2</sup> and Huajie Li <sup>1</sup>

<sup>1</sup> School of Environmental & Safety Engineering, Changzhou University, Changzhou 213164, China; duerdeng@cczu.edu.cn (E.D.); licczu1995@163.com (J.L.); siqizhou1996@163.com (S.Z.); hjxy19981021@outlook.com (H.L.)

<sup>2</sup> School of Environment, Tsinghua University, Beijing 100084, China; x.liu@tsinghua.edu.cn

\* Correspondence: miaoli@tsinghua.edu.cn; Tel.: +86-10-6278-3085

Received: 3 August 2018; Accepted: 10 September 2018; Published: 13 September 2018



**Abstract:** Environmental problems caused by UV filters, a group of emerging contaminants, have attracted much attention. The removal of two typical UV filters benzophenone (BP) and 4,4'-dihydroxy-benzophenone (HBP) in water was investigated by the UV/H<sub>2</sub>O<sub>2</sub> process. The response surface methodology (RSM) and central composite design (CCD) were applied to investigate the effects of the process parameters on the degradation rate constants, including the initial contaminant concentration, H<sub>2</sub>O<sub>2</sub> dose, and UV light intensity. BP is more easily degraded by the UV/H<sub>2</sub>O<sub>2</sub> process. Both processes followed pseudo-first-order kinetics. The results obtained with the built RSM model are in accordance with the experimental results (adjusted coefficients  $R^2(\text{adj}) = 0.9835$  and  $0.9778$  for BP and HBP, respectively). For both processes, the initial contaminant concentration (exerting a negative effect) were the most important factors controlling the degradation, followed by H<sub>2</sub>O<sub>2</sub> dose and UV intensity (exerting positive effects). A total of 15 BP degradation products and 13 HBP degradation products during the UV/H<sub>2</sub>O<sub>2</sub> process were identified by LC/MS and GC/MS. A series of OH radical irritated reactions, including hydroxylation, carboxylation, and ring cleavage, led to the final degradation of BP and HBP. Degradation pathways of BP and HBP were also proposed. On the whole, this work is a unique contribution to the systematic elucidation of BP and HBP degradation by the UV/H<sub>2</sub>O<sub>2</sub> process.

**Keywords:** emerging contaminants; benzophenone-type UV filters; UV/H<sub>2</sub>O<sub>2</sub>; advanced oxidation process; response surface methodology (RSM); degradation products

## 1. Introduction

Organic UV filters have been extensively used in sunscreens for skin protection. The organic UV filters and their metabolites may flow into rivers or lakes due to the emission through direct discharge (washing) or indirect discharge (sewage plant effluents) [1,2]. Many UV filters have been detected in the aqueous environment, including 2,4-dihydroxy benzophenone (2,4-DBP), benzophenone-3 (BP3), 2-phenylbenzimidazole-5-sulfonic acid (UV-T), octyl methoxycinnamate (OMC), and octocrylene [3,4]. Most of the organic UV filters are lipophilic compounds and tend to accumulate in soils and sediments of the aqueous environment, as well as in the food chain (e.g., fish, birds, mammals) [5]. The accumulation of UV filters in organisms has become a major concern, because many UV filters and their metabolites show the apparent endocrine disruption and the hormonal effects, both in vitro and in vivo [6,7].

Benzophenone (BP) and 4,4'-dihydroxy-benzophenone (HBP), two type of benzophenone-type UV filters, are widely detected in sewage and other environmental media across the world, such as

United States, Japan, and Switzerland [5,8–12]. There are reports that the concentration of BP reached 250 ng/L in wastewater [13]. The potential risks resulting from the occurrence of BP and HBP must not be overlooked.

Advanced oxidation processes (AOPs) are a series of processes that can generate hydroxyl radicals to efficiently degrade organic pollutants in contaminated water [4,14,15]. The UV/H<sub>2</sub>O<sub>2</sub> system is a type of AOP, in which hydrogen peroxide (H<sub>2</sub>O<sub>2</sub>) is added in the presence of UV light to generate hydroxyl radicals [16–18]. It is found that the UV/H<sub>2</sub>O<sub>2</sub> process can remove a large range of organic pollutants, including cyanobacterial toxins [19], diclofenac [20], amoxicillin [21], and other emerging contaminants [22–24].

Benzophenone-type UV filters are usually the hardly biodegradable substances [25]. There are over 20 benzophenone-type UV filters, including HBP, BP, benzophenone-2, benzophenone-3 (BP3), benzophenone-4, benzophenone-5, and benzophenone-9. Among them, BP3 is the dominant UV filter and the most-frequently detected in the aquatic environment [26,27]. Many reported works have focused on the occurrence, transformation, and fate of BP3 [28–30]. The removal, degradation mechanism, and ecotoxicity of BP3 by different treatment processes were assessed, such as UV/H<sub>2</sub>O<sub>2</sub> [31], ozone [32], fungal [33], chlorination [34,35], and activated persulfate [36,37]. In addition, the removal of other benzophenone-type UV filters, including BP2, BP4, and BP9, were also evaluated by different AOPs [38–43].

BP, as a basic benzophenone-type substance with the simplest structure, is the important precursor for the production of other benzophenone-type UV filters. However, there are few reports on the removal of BP by photocatalysis and ozonation [44,45]. Chen [46] and Katsuhiko [47] investigated the biodegradation and fate of BP in aquatic environments and the activated sludge of a sewage treatment plant. It took a relatively long time for microbes to degrade a certain concentration of BP due to the toxic effect of BP. HBP is the di-hydroxyl addition product of BP. To date, research examining about the removal of BP and HBP by the UV/H<sub>2</sub>O<sub>2</sub> process is rarely reported. The degradation behavior and characteristics of BP by AOPs have great reference value for the treatment and control of wastewater containing benzophenone-type UV filters.

The primary purpose of this research is to explore the degradation of two UV filters BP and HBP in water by the UV/H<sub>2</sub>O<sub>2</sub> advanced oxidation process. The response surface methodology (RSM) analysis combined with the experimental design is used to investigate the main factors of the UV/H<sub>2</sub>O<sub>2</sub> process. Additionally, the degradation intermediates are identified by an LTQ-Orbitrap high-resolution mass spectrometer and GC-MS. Through these analyses, combined with the chemical structure analysis, degradation mechanisms of BP and HBP by the UV/H<sub>2</sub>O<sub>2</sub> process are also proposed.

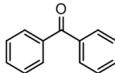
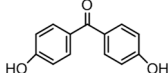
## 2. Materials and Methods

### 2.1. Chemicals and Reagents

BP and HBP were purchased from Energy Chemical Reagent (Shanghai, China). The relevant physical and chemical properties are shown in Table 1. Methanol (HPLC grade) was obtained from Sigma-Aldrich, Inc. (St. Louis, MO, USA). Hydrochloric acid, sodium hydroxide, and hydrogen peroxide (H<sub>2</sub>O<sub>2</sub> 30% w/w) were all of analytical grade. All solutions were prepared using ultrapure water (resistivity 18.3 mΩ·cm) from a Milli-Q water purification system (Millipore, Burlington, MA, USA). An Oasis HLB cartridge (Waters, 500 mg, 6 cc, Milford, MA, USA) was used for the solid phase extraction (SPE) pretreatment. A silylation reagent (Ekear, Shanghai, China), containing N,O-bis(trimethylsilyl)trifluoroacetamide and trimethylchlorosilane (BSTFA/TMCS, 99:1), was used for the GC derivatization.

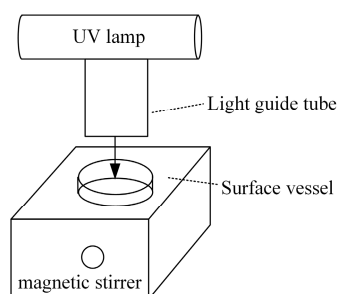


**Table 1.** Properties of benzophenone (BP) and 4,4'-dihydroxy-benzophenone (HBP).

Properties	BP	HBP
Name	Benzophenone	4,4'-dihydroxy-benzophenone
CAS Number	119-61-9	611-99-4
Molecular Formula	C <sub>13</sub> H <sub>10</sub> O	C <sub>13</sub> H <sub>10</sub> O <sub>3</sub>
Molecular Weight	182.2179	214.2167
Partition coefficient (Log P)	3.18	2.55
Molar Refractivity	56.0 ± 0.3	59.8 ± 0.3
Chemical Structure		

## 2.2. Photoreactor and Experimental Tests

The photodegradation experiment was performed in a glass photoreactor (200-mL volume, 10-cm diameter), as shown in Figure 1. A lamp emitting at 254 nm (75 W, Philips, Shanghai, China) was hung over the glass photoreactor. A stir bar was kept in the reactor for the solution mixing. The compound solution and H<sub>2</sub>O<sub>2</sub> were added into the reactor. The compound solution and H<sub>2</sub>O<sub>2</sub> were added in a range of concentrations to the photoreactor. The range of BP/HBP concentration is 4 to 50 mg·L<sup>-1</sup>, while the range of H<sub>2</sub>O<sub>2</sub> dose is 0.1–0.5 mmol·L<sup>-1</sup>. The UV light was then turned on to start the degradation reaction. BP and HBP samples were collected at set intervals. The distance between the UV lamp and the water surface was adjusted manually for various UV intensities, which were determined by an ultraviolet meter (Model UV-B, Photoelectric Instrument Factory of Beijing Normal University).

**Figure 1.** Experimental setup.

## 2.3. Compounds Determination

Quantitative analyses of BP and HBP were carried out by liquid chromatography (LC-100, Wu Feng, China), which was equipped with an HPLC C18 column (4.6 × 150 mm, 5 μm, LK Tech). The mobile phase was 60% methanol and 40% water with 5 mM ammonium acetate. The other optimized conditions were as follows: a flow velocity of 1.0 mL·min<sup>-1</sup>, an isocratic elution, and a UV wavelength of 264 nm. Under the HPLC conditions, the compound peak with high resolution was obtained for quantitative analyses. The determination error was less than 5%.

## 2.4. Degradation Products Identification

Water samples were collected at set intervals during the process and later mixed together. Before the LC-MS and GC-MS analysis, water samples were pretreated according to an SPE procedure developed and optimized by our research group [40].

Mass spectrum data was acquired through the acquisition of parent ions combined with the analysis of diagnostic product ions on a hybrid LTQ-Orbitrap (Thermo Scientific, Waltham, MA, USA). The other MS conditions were as follows: negative mode, data-dependent acquisition (DDA),

a dynamic exclusion of 5 s, and a collision energy (CE%) of 45 eV. The chromatography separation was performed with a Polar-RP C<sub>18</sub> column (Welch Ultimate, 100 × 2.1 mm, 3.0 μm).

A GC-MS (QP-2010, Shimadzu, Kyoto, Japan) equipped with a capillary column (DB-5, 30 m × 0.5 mm × 0.5 mm) was used to identify the degradation products, such as small molecular organic acids. Before the GC-MS analysis, water samples were prepared through freeze-drying and sequent derivatization by a BSTFA/TMCS reagent at 70 °C [48]. Sample preparation was repeated three times for LC-MS and GC-MS analysis.

## 2.5. CCD Experimental Design and RSM Analysis

RSM is a useful tool for the exploration of the relationship between explanatory variables and response variables [49,50]. Currently, RSM is extensively used for experimental design, model building, and parameter evaluation and optimization [51–53]. Central composite design (CCD) is an experimental design, useful in response surface methodology, for building a RSM model. In this research, RSM and central composite design (CCD) were applied to investigate the contaminant degradation by the UV/H<sub>2</sub>O<sub>2</sub> process, as shown in Table 2.

Design Expert 7.1 software (student evaluation version) (Stat-Ease, Minneapolis, MN, USA) was applied for the experimental design, RSM analysis, and RSM model construction. Three factors were selected to evaluate the influence of the operating parameters, including the UV light intensity ( $x_1$ ), initial contaminant concentration ( $x_2$ ), and H<sub>2</sub>O<sub>2</sub> dose ( $x_3$ ). A total of 40 runs were performed in the experiment, including 20 runs for BP, and 20 runs for HBP. The experiment was repeated three times to obtain the average. Pseudo-first-order rate constants for a 30 min UV radiation ( $K_{BP1}$ ,  $K_{HBP}$ ) were taken as the response variables, calculated by Equation (1).

$$\ln\left(\frac{C}{C_0}\right) = -K \times t \quad (1)$$

where  $C_0$  and  $C$  are the contaminant concentration at 0, and  $t$  min in mg·L<sup>−1</sup>,  $K$  is the first-order rate constant in min<sup>−1</sup>, and  $t$  the reaction time in min.

For the statistical calculation, the variables  $x_i$  were coded to  $X_i$  through Equation (2):

$$X_i = \frac{x_i - x_0}{\delta x} \quad (2)$$

where  $X_i$  is the dimensionless value of an independent variable,  $x_i$  is the real value of the variable,  $x_0$  is the real value of the variable at the center point, and  $\delta x$  represents the step change [54].

## 3. Results and Discussion

### 3.1. BP and HBP Degradation by the UV/H<sub>2</sub>O<sub>2</sub> Process

The removal of BP and HBP with three different initial contaminant concentrations in 30 min was compared, as shown in Figure 2. The other reaction conditions included a UV intensity of 900 μW·cm<sup>−2</sup> and an H<sub>2</sub>O<sub>2</sub> concentration of 0.30 mmol·L<sup>−1</sup>. The removal of HBP was only 37.7%, while the BP removal was as high as 74.9% in 30 min with an initial contaminant concentration of 13.8 mg·L<sup>−1</sup>. It is evident that the removal of BP was much higher than that of HBP under the same degradation conditions, which means that BP is more easily degraded by the UV/H<sub>2</sub>O<sub>2</sub> process. HBP is the di-hydroxyl addition product of BP. After a hydroxyl group is added on the ring of BP, the steric hindrance effect possibly prevents the further addition of hydroxyl radical on the ring [55], which makes the degradation of HBP by the UV/H<sub>2</sub>O<sub>2</sub> process more difficult.

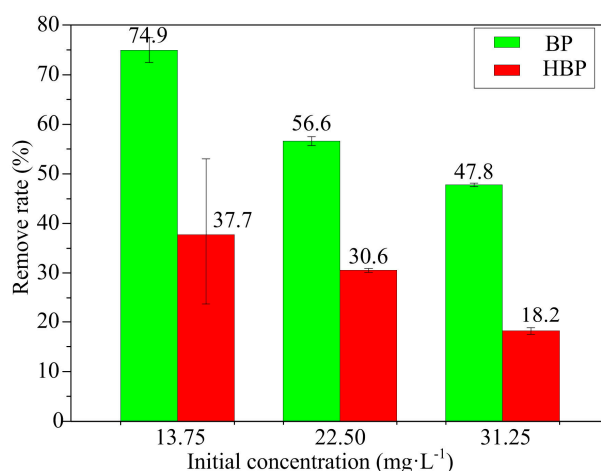


**Figure 2.** BP and HBP removal by the UV/H<sub>2</sub>O<sub>2</sub> process.

Pseudo first-order reaction kinetics was also used to describe the UV/H<sub>2</sub>O<sub>2</sub> process, as shown in Figure 3. The experimental conditions were as follows: a UV intensity of 900  $\mu\text{W}\cdot\text{cm}^{-2}$ , an H<sub>2</sub>O<sub>2</sub> concentration of 0.30 mmol·L<sup>-1</sup>, and an initial BP/HBP concentration of 22.5 mg·L<sup>-1</sup>. The reaction rate constants of BP and HBP are 0.025 and 0.012, respectively. Figure 3 shows that pseudo-first-order reaction kinetics was successfully fitted with test results ( $R^2(\text{adj})$  0.991 and 0.982), according to the kinetic model Equation (1).

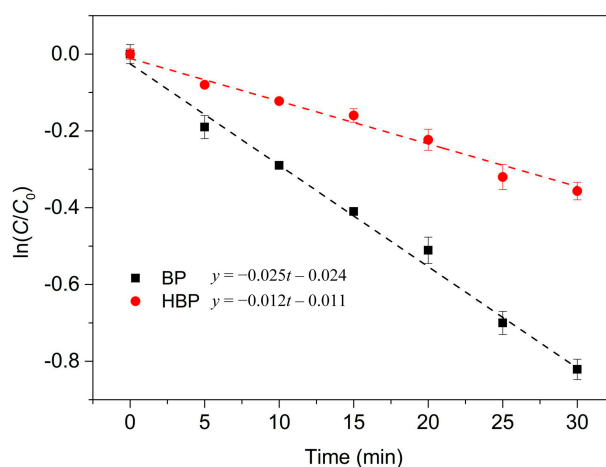


**Figure 3.** Degradation kinetics of BP and HBP by the UV/H<sub>2</sub>O<sub>2</sub> process.

### 3.2. Established RSM Model and Its Validation

All runs were performed according to the CCD experimental design. Pseudo-first-order reaction kinetics was used to fit the experimental results of every run. The regression coefficients ( $R^2 > 0.95$ ) show that the degradation reactions were in good agreement with the pseudo-first-order reaction kinetics at different degradation parameters. Pseudo-first-order rate constants were calculated by Equation (1), summarized in Table 2.

Table 2. Expert design together with the observed experimental data.

Run	UV Light $x_1$ ( $\mu\text{W}\cdot\text{cm}^{-2}$ )	Initial Concentration $x_2$ ( $\text{mg}\cdot\text{L}^{-1}$ )	$\text{H}_2\text{O}_2$ Concentration $x_3$ ( $\text{mmol}\cdot\text{L}^{-1}$ )	First-Order Degradation Rate Constant ( $\text{min}^{-1}$ )	
				$K_{\text{BP}}$ ( $\text{min}^{-1}$ )	$K_{\text{HBP}}$ ( $\text{min}^{-1}$ )
1	1400	5.00	0.10	0.050	0.023
2	900	22.5	0.20	0.020	0.010
3	400	5.00	0.50	0.069	0.037
4	900	22.5	0.30	0.027	0.012
5	400	5.00	0.10	0.015	0.008
6	900	31.3	0.30	0.025	0.007
7	900	22.5	0.30	0.031	0.013
8	400	40.0	0.10	0.003	0.004
9	900	22.5	0.30	0.029	0.012
10	900	22.5	0.40	0.032	0.015
11	900	22.5	0.30	0.023	0.012
12	400	40.0	0.50	0.013	0.005
13	1150	22.5	0.30	0.033	0.014
14	900	22.5	0.30	0.030	0.012
15	650	22.5	0.30	0.021	0.011
16	1400	5.00	0.50	0.131	0.065
17	900	22.5	0.30	0.025	0.012
18	1400	40.0	0.50	0.036	0.008
19	1400	40.0	0.10	0.013	0.002
20	900	13.8	0.30	0.047	0.015

Based on the results obtained in each run, an RSM model was constructed to explain the relationship between the reaction parameters and the results, as follows:

$$K_{\text{BP}} = 0.0280 + 0.0160X_1 - 0.0250X_2 + 0.0210X_3 - 0.0080X_1X_2 + 0.0050X_1X_3 - 0.0130X_2X_3 - 0.0069X_1^2 + 0.0310X_2^2 - 0.0100X_3^2 \quad (3)$$

$$K_{\text{HBP}} = 0.0120 + 0.0053X_1 - 0.014X_2 + 0.0093X_3 - 0.0054X_1X_2 + 0.0019X_1X_3 - 0.0082X_2X_3 + 0.0036X_1^2 - 0.0016X_2^2 + 0.0052X_3^2 \quad (4)$$

Considering only the first-order effect in Equation (3),  $X_2$  has a high coefficient of 0.025, followed by  $X_3$  (0.021) and  $X_1$  (0.016). This means  $X_2$  (the initial BP concentration) has the most important effect on rate constants and therefore inhibits the observed rate constant. From the above polynomial, it can be readily seen that a high synergetic effect of  $X_2X_3$  (0.013) decreases the rate constant. The similar observation can also be seen in Equation (4).

After the models are built, the analysis of variance (ANOVA) is used to assess the significance of each term, and the robustness of the RSM model. Table 3 shows the summary of the analysis outcomes, including the estimated effects, and the ANOVA of the models with coded units. F-values of 127.0 (BP model) and 93.9 (HBP model) imply that the two models are of significance. There is a less than 0.01% chance for the BP and HBP models that these large “Model F-values” could occur due to noise. The degree of significance of each term is represented by its  $P$ -value. A  $P$ -value less than 0.05 indicates the significance of the model terms, while the value higher than 0.05 explains that the model terms are of insignificance [56].

**Table 3.** Analysis of variance (ANOVA) for BP and HBP degradation model.

Terms	Sum of Squares	BP			Sum of Squares	HBP		
		Mean Square	F-Value	P-Value		Mean Square	F-Value	P-Value
Model	$1.412 \times 10^{-3}$	$1.549 \times 10^{-3}$	127.01	<0.0001	$3.668 \times 10^{-3}$	$4.076 \times 10^{-4}$	93.92	<0.0001
$X_1$	$2.194 \times 10^{-3}$	$2.194 \times 10^{-3}$	179.87	<0.0001	$2.404 \times 10^{-4}$	$2.404 \times 10^{-4}$	55.38	<0.0001
$X_2$	$5.223 \times 10^{-3}$	$5.223 \times 10^{-3}$	428.25	<0.0001	$1.652 \times 10^{-3}$	$1.652 \times 10^{-3}$	380.65	<0.0001
$X_3$	$3.582 \times 10^{-3}$	$3.582 \times 10^{-3}$	293.74	<0.0001	$7.380 \times 10^{-4}$	$7.380 \times 10^{-4}$	170.04	<0.0001
$X_1X_2$	$5.072 \times 10^{-4}$	$5.072 \times 10^{-4}$	41.59	<0.0001	$2.365 \times 10^{-4}$	$2.365 \times 10^{-4}$	54.50	<0.0001
$X_1X_3$	$2.030 \times 10^{-4}$	$2.030 \times 10^{-4}$	16.65	0.0022	$3.003 \times 10^{-5}$	$3.003 \times 10^{-5}$	6.92	0.0251
$X_2X_3$	$1.303 \times 10^{-3}$	$1.303 \times 10^{-3}$	106.84	<0.0001	$5.396 \times 10^{-4}$	$5.396 \times 10^{-4}$	124.32	<0.0001
$X_1^2$	$8.762 \times 10^{-6}$	$8.762 \times 10^{-6}$	0.72	0.4165	$2.413 \times 10^{-6}$	$2.413 \times 10^{-6}$	0.56	0.4731
$X_2^2$	$1.742 \times 10^{-4}$	$1.742 \times 10^{-4}$	14.28	0.0036	$4.803 \times 10^{-7}$	$4.803 \times 10^{-7}$	0.11	0.7462
$X_3^2$	$1.962 \times 10^{-5}$	$1.962 \times 10^{-5}$	1.61	0.2335	$5.038 \times 10^{-6}$	$5.038 \times 10^{-6}$	1.16	0.3066
Lack of Fit	$7.843 \times 10^{-5}$	$1.569 \times 10^{-5}$	1.65	0.2978	$1.962 \times 10^{-5}$	$1.962 \times 10^{-5}$	1.61	0.2335

As for the two models, UV intensity ( $X_1$ ), initial contaminant concentration ( $X_2$ ), and  $H_2O_2$  dose ( $X_3$ ) are the significant model terms and have a statistically significant effect upon the degradation rate constants ( $P$ -value < 0.05). Their interaction terms between the three factors, including  $X_1X_2$  and  $X_2X_3$ , are also significant terms. However, the terms' square interactions ( $X_1^2$ ,  $X_2^2$ , and  $X_3^2$ ) do not exhibit a statistically significant effect.

The regression coefficients ( $R^2$ ) indicates how much of the variability in the data is accounted for by the model.  $R^2$ (adj) values of the BP and HBP models are 0.9835 and 0.9778, respectively. These imply that 98.35% and 97.78% of the variations for BP/HBP degradation rate constants are explained by the independent variables, and only about 1.65% and 2.22% of the variations are not explained by the model. The F-values for the lack-of-fit test of the BP and HBP models are 1.65 and 4.50, respectively, which means the lack-of-fit is significant relative to the pure error. The results illustrate that the two models adequately match the UV/ $H_2O_2$  process and can serve to investigate the experimental data space.

### 3.3. Analysis of the Response Surface Models

Response surface contour plots of BP and HBP degradation are shown in Figure 4, in which the inner effects of three variables on the rate constant are presented. These charts show the strong interaction among UV light intensity, initial contaminant concentration, and  $H_2O_2$  dose, which had a statistically significant effect on the UV/ $H_2O_2$  degradation. The single effects on the rate constants of BP and HBP degradation are also shown in Figure A1.



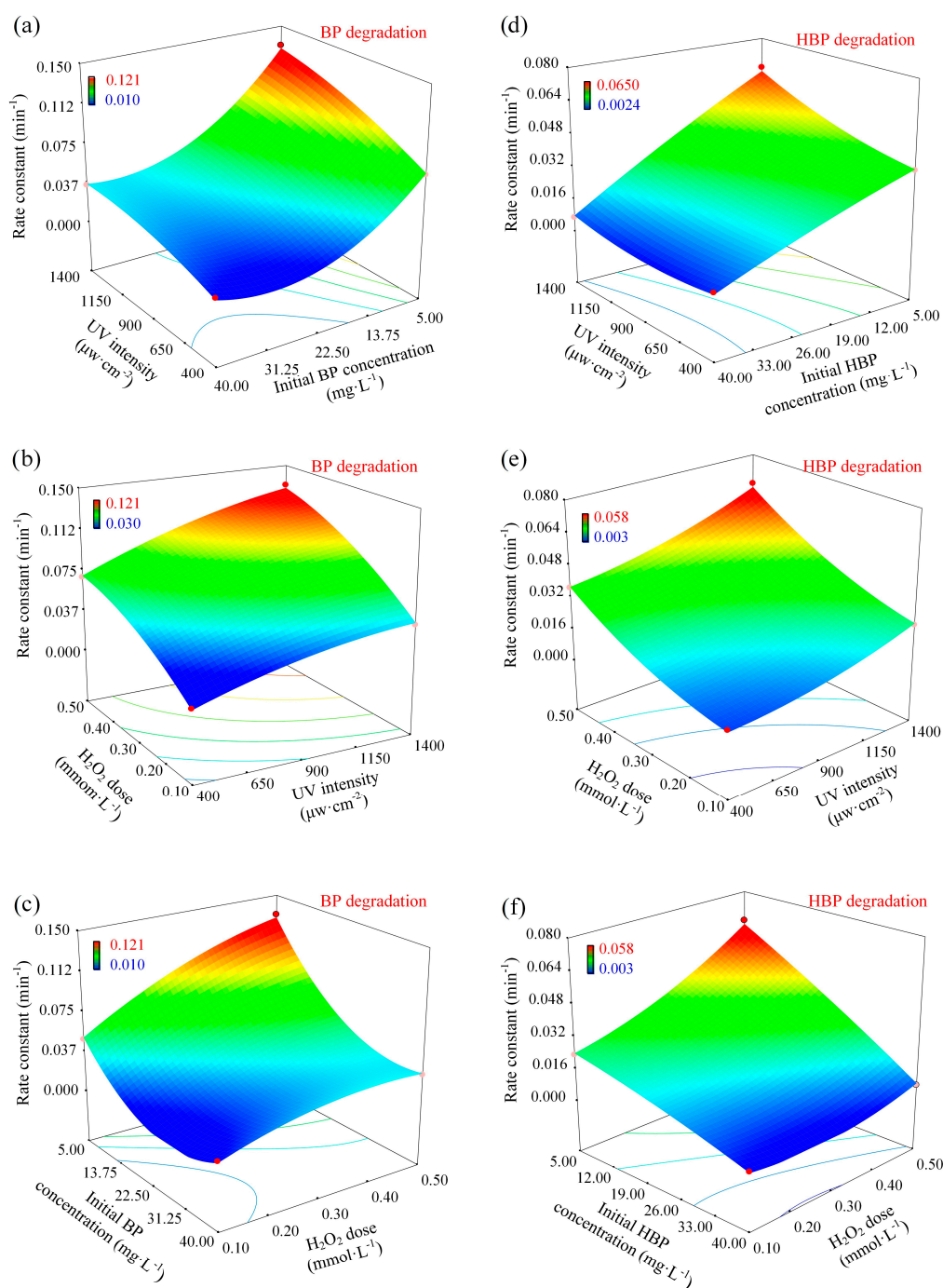


**Figure 4.** Response surface plots that present the inner effects of three variables on the rate constant ( $K$ ): BP and HBP models. (a) Initial BP concentration and UV intensity; (b) H<sub>2</sub>O<sub>2</sub> dose and UV intensity; (c) initial BP concentration and H<sub>2</sub>O<sub>2</sub> dose; (d) initial HBP concentration and UV intensity; (e) H<sub>2</sub>O<sub>2</sub> dose and UV intensity; (f) initial HBP concentration and H<sub>2</sub>O<sub>2</sub> dose. (Colors represent the strength of rate constant from the low (blue) to the medium (green) and to the large (red)).

The results show that UV light intensity and H<sub>2</sub>O<sub>2</sub> dose have a positive effect on the rate constant (Figure 4a–d; Figure A1a,e). In other words, a higher UV intensity and H<sub>2</sub>O<sub>2</sub> dose yields a higher rate constant. UV intensity is a critical factor for the OH radical production, which is primarily responsible for the contaminant degradation. The increase in UV photons in the solution causes an increase in OH radical concentration, thereby accelerating the degradation process.

It is also evident that  $\text{H}_2\text{O}_2$  is an essential source for the OH radical production (Figure A1c,f). The addition of  $\text{H}_2\text{O}_2$  could produce more OH radicals to accelerate the degradation process. Similar findings were also observed during BP3 and ibuprofen degradation by the UV/ $\text{H}_2\text{O}_2$  process [31,57]. However, previous studies explained that the excessive addition of  $\text{H}_2\text{O}_2$  shows an adverse effect on the removal, due to the scavenger effect of  $\text{H}_2\text{O}_2$  on OH radicals [51,58]. In the current test,  $\text{H}_2\text{O}_2$  dose shows a positive effect on the rate constant in the range of 0.1 to 0.5  $\text{mmol}\cdot\text{L}^{-1}$ , which means  $\text{H}_2\text{O}_2$  concentration has not reached the inhibition zone.

The initial BP and HBP concentrations illustrate the adverse effect on the rate constant (Figure 4c,f; Figure A1b,e). In other words, a higher initial contaminant concentration could inhibit the degradation process. BP and HBP are both efficient UV filters and could absorb UV photons in solution. With the increasing of initial contaminant concentration, the contaminants could absorb more UV photons, which reduces the production of OH radicals inspired by UV photons, thereby further decreasing the degradation efficiency [31]. Moreover, the robustness of the models was also investigated by the diagnostic plots (Figure 5). The data points nearly scattering along a straight line in Figure 5 indicates that the predicted values in the models are equal to the actual values.

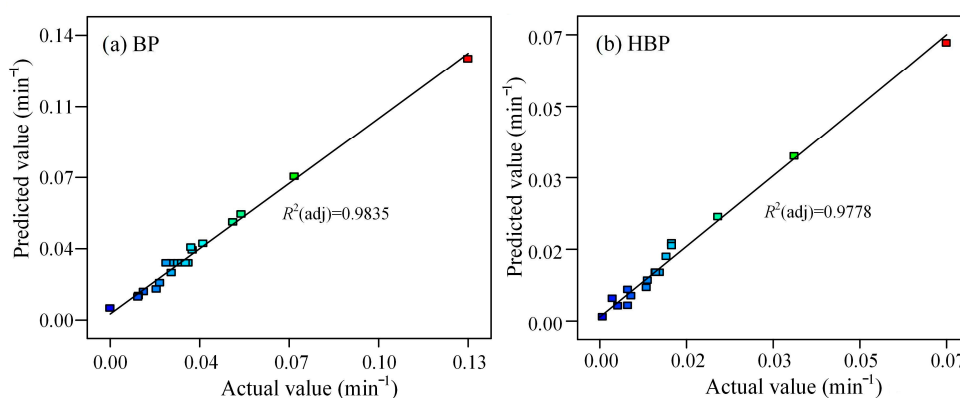


**Figure 5.** Actual values versus predicted values obtained from the estimated model. (Colors represent the strength of rate constant from the low (blue) to the medium (green) and to the large (red))

The effects of three parameters on degradation can be compared with the help of perturbation plots (Figure 6). The plots were obtained at UV intensity of  $900\ \mu\text{W}\cdot\text{cm}^{-2}$ , the initial BP/HBP concentration  $22.5\ \text{mg}\cdot\text{L}^{-1}$  and  $\text{H}_2\text{O}_2$  dose of  $0.30\ \text{mmol}\cdot\text{L}^{-1}$ . The steep curvatures indicated that the response of BP/HBP degradation rate constant was sensitive to these three factors [59]. The degradation was largely controlled by the initial BP/HBP concentration, followed by  $\text{H}_2\text{O}_2$  dose and UV intensity.

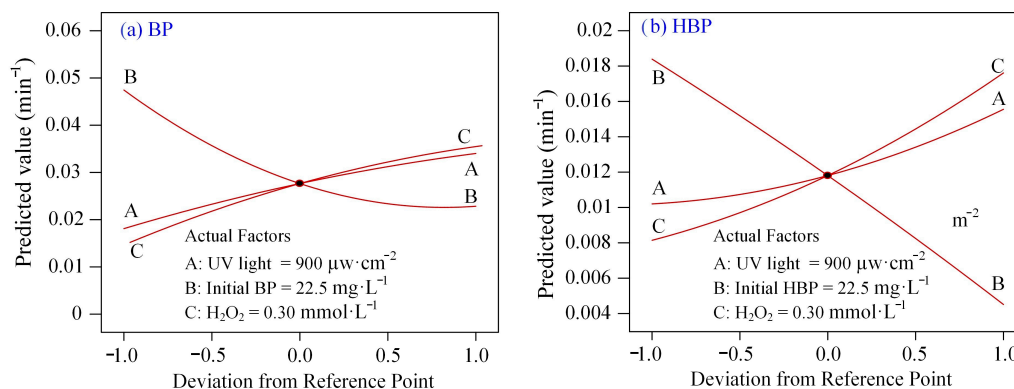


**Figure 6.** Perturbation graphs for (a) BP degradation and (b) HBP degradation.

Based on RSM analysis above, the maximum degradation rate constants of BP and HBP were optimized. The optimized conditions were as follows: a UV light intensity of  $1150 \mu\text{W}\cdot\text{cm}^{-2}$ , an  $\text{H}_2\text{O}_2$  dosage of  $0.40 \text{ mmol}\cdot\text{L}^{-1}$ , and an initial BP/HBP concentration of  $13.8 \text{ mg}\cdot\text{L}^{-1}$ . The predicted maximum rate constants of BP and HBP degradation were  $0.068$  and  $0.032 \text{ min}^{-1}$ , respectively. The results of the further experimental test with the optimized parameters were in good agreement with the predicted values. It was concluded that RSM analysis is a powerful strategy to investigate and optimize the process parameters [60–62].

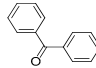
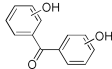
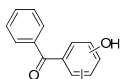
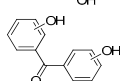
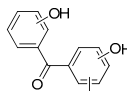
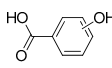
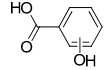
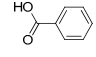
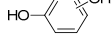
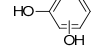
### 3.4. Degradation Mechanism of BP

Degradation products could be produced during the UV/ $\text{H}_2\text{O}_2$  process. A total of 15 products (including isomers) were identified, including 9 compounds by LTQ-Orbitrap and 6 compounds by GC-MS, as summarized in Tables 4 and 5, respectively. Chromatogram (EIC), and  $\text{MS}^2$  spectra of BP and its products identified by LTQ-Orbitrap are illustrated in Figures 7 and A2, Figures A3–A6, respectively.

BP was detected with an appearance time of 13.96 min and the molecular ion at  $183.0804 m/z$  in a positive mode (Figure 7a). In particular, one structural diagnostic ion was evidenced at  $106.04 m/z$ , formed from the loss of a phenyl group ( $-\text{C}_6\text{H}_5$ , 77 dalton(Da)).

One degradation product at  $[\text{M}-\text{H}]^-$   $197.0608 m/z$  with an empirical formula of  $\text{C}_{13}\text{H}_{10}\text{O}_2$  was determined with an appearance time of 13.19 min in a negative mode and attributed to the mono-hydroxylated BP (entitled BP-OH, Figure 7b).  $\text{MS}^2$  spectrum presents one product ion at  $121.03 m/z$ , also attributed to the detachment of one phenyl group. Hydroxyl (OH) radicals could be attached and added to different sites on the aromatic ring of BP. However, the specific position cannot be distinguished owing to the limitation of the current HRMS technology.

**Table 4.** Molecular formula and properties of BP and its degradation products.

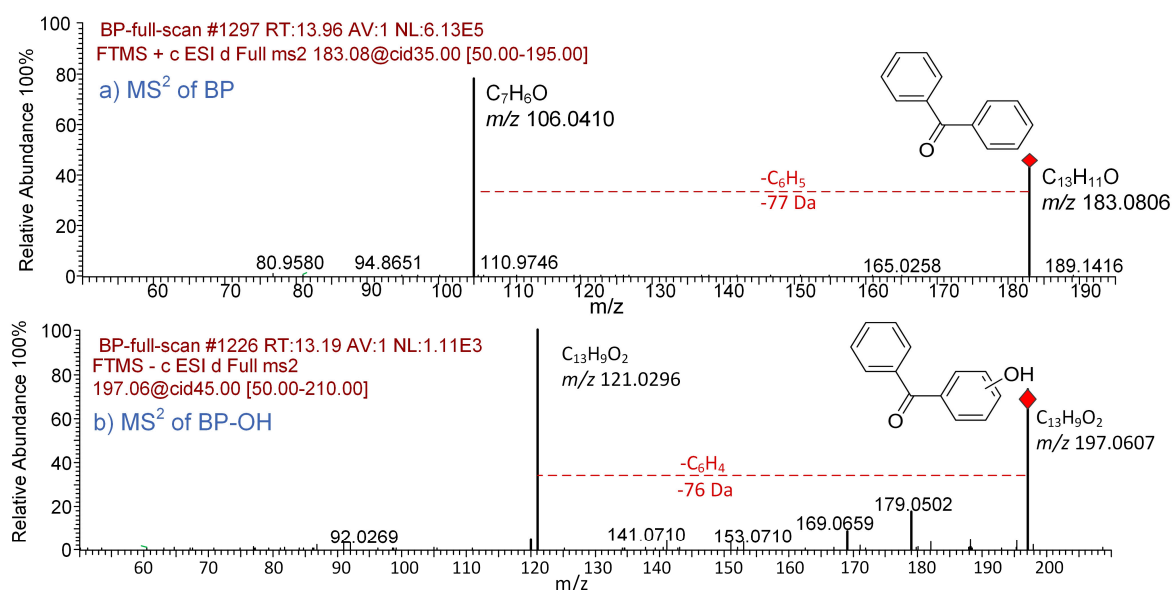
Code	Retention Time (min)	Molecular Formula	Theoretical $m/z$	Molecular Ions Measured $m/z$	$\Delta$ ppm	Structure
BP	13.96	$\text{C}_{13}\text{H}_{10}\text{O}$	183.0804 *	183.0806	1.10	
BP-OH	13.19	$\text{C}_{13}\text{H}_{10}\text{O}_2$	197.0608	197.0608	0.25	
BP-2OH-a	15.34	$\text{C}_{13}\text{H}_{10}\text{O}_3$	213.0557	213.0556	0.47	
BP-2OH-b	16.89	$\text{C}_{13}\text{H}_{10}\text{O}_3$	213.0557	213.0555	0.94	
BP-3OH	14.27	$\text{C}_{13}\text{H}_{10}\text{O}_4$	229.0506	229.0505	0.44	
Pr138-a	2.58	$\text{C}_7\text{H}_6\text{O}_3$	137.0244	137.0244	0.18	
Pr138-b	6.42	$\text{C}_7\text{H}_6\text{O}_3$	137.0244	137.0245	0.73	
Benzoic acid	12.43	$\text{C}_7\text{H}_6\text{O}_2$	121.0295	121.0295	0.33	
Pr110-a	8.62	$\text{C}_6\text{H}_6\text{O}_2$	109.0295	109.0296	0.91	
Pr110-b	12.93	$\text{C}_6\text{H}_6\text{O}_2$	109.0295	109.0298	2.75	

\* All of the molecular ions are detected in the negative mode, except BP detected in the positive mode; “Pr” is the abbreviation of “product”.

Table 5. Degradation products of BP detected by GC/MS.

Products	Molecular Weight	CAS Number	GC Retention Time (min)	Molecular Structure
Glycolic acid (2TMS *)	220	33581-77-0	5.42	
Oxalic acid (2TMS)	234	18294-04-7	5.81	
Malonic acid (2TMS)	248	18457-04-0	6.29	
2-Butenedioic acid (2TMS)	260	23508-82-9	6.91	
Tartronic acid (3TMS)	336	38165-93-4	7.40	
Malic acid (3TMS)	350	38166-11-9	7.92	

\* TMS in the product name stands for a trimethylsilyl group.

Figure 7. MS<sup>2</sup> spectra of BP and its degradation product obtained by LTQ-Orbitrap. (a) BP, (b) BP-OH.

More than one OH radical could further be added to the ring to yield di-hydroxylated or tri-hydroxylated products [40]. Two di-hydroxylated products, named BP-2OH-a and BP-2OH-b, were found at  $[M-H]^-$  213.0556  $m/z$  with a retention time of 15.34 min and  $[M-H]^-$  213.0555  $m/z$  with a retention time of 16.89 min (Table 4, Figure A2), respectively. Both BP-2OH-a and BP-2OH-b are the isomers of HBP. In fact, hydroxyl addition reaction is very common in AOPs and biological oxidation processes. Pablo et al. found the occurrence of HBP during BP-3 degradation by ozonation process [63] and microbial oxidation in soil [64]. Moreover, one tri-hydroxylated product (BP-3OH) was also determined at  $[M-H]^-$  229.0505  $m/z$  with a retention time of 14.27 min (Figure A3).

OH radicals will attack the ketone group of BP and its addition products, which leads to the break of the C–C bond adjacent to the ketone group and the generation of the formyl group. The formyl group could be oxidized to the carboxyl group. With the successive attack by OH radicals, a series of products containing a mono-benzene ring were produced, including Pr138-a, Pr138-b, benzoic acid, Pr110-a, and Pr110-b (Table 4 and Figures A4–A6).

In the later degradation period of compounds containing aromatic rings, OH radicals could cleave the aromatic ring and produce small molecular organic acids. Several reports illustrate that the common organic acids, such as 1,2-dihydroxypropane, glycolic acid, pyruvic acid, formic acid, and propane-dioic acid, usually appear during the degradation of ibuprofen and dimethyl phthalate by the UV/H<sub>2</sub>O<sub>2</sub> process [40,48,57]. In this study, six organic acids were determined, including glycolic acid, oxalic acid, malonic acid, 2-butenedioic acid, tartronic acid, and malic acid (Table 5).

Therefore, a possible reaction pathway for the BP degradation by the UV/H<sub>2</sub>O<sub>2</sub> process is proposed (Figure 8). A series of OH radical irritated reactions take place during the process, including hydroxylation, carboxylation, and ring cleavage, which result in the degradation of BP and finally the formation of CO<sub>2</sub> and H<sub>2</sub>O.



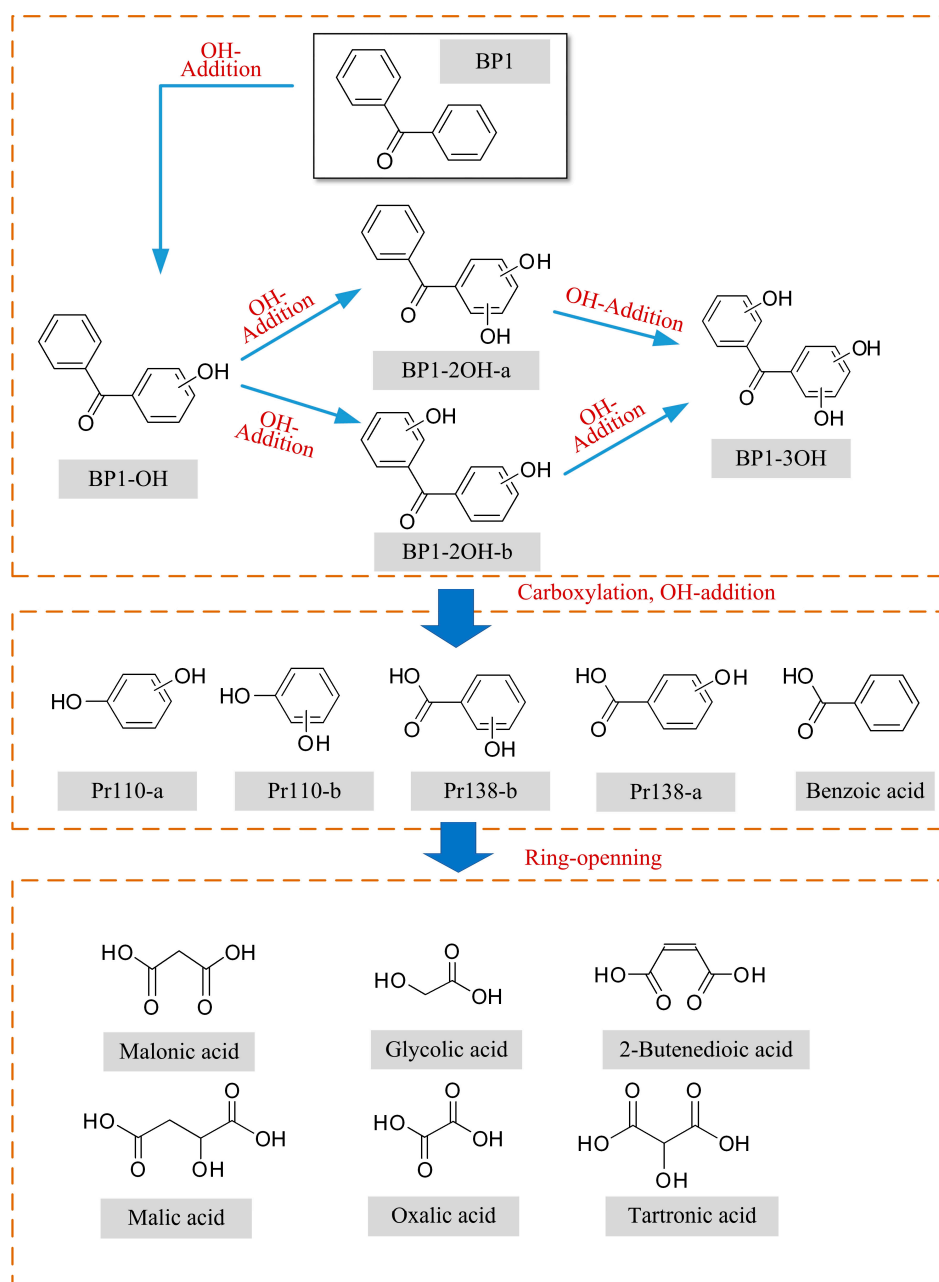
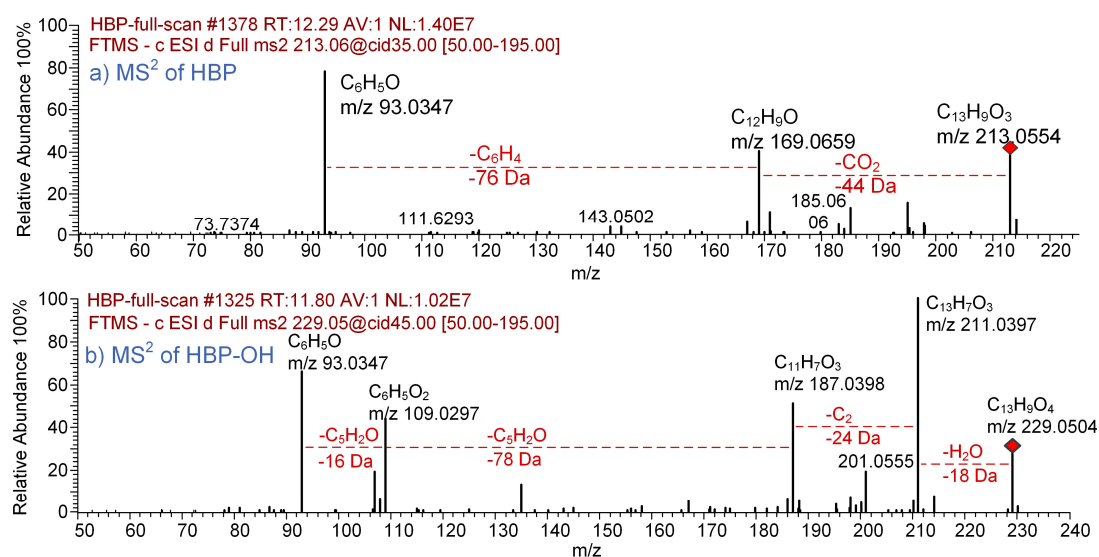


Figure 8. Proposed pathway of the BP degradation by the UV/H<sub>2</sub>O<sub>2</sub> process.

### 3.5. Degradation Mechanism of HBP

Both BP and HBP have the homologous benzophenone-type structure. The only difference is that HBP holds two hydroxyl groups on the aromatic rings. In this research, 13 HBP products were detected, including seven compounds by LTQ-Orbitrap and six compounds by GC-MS, shown and listed in Figure 9 and Tables 6 and 7. HBP was determined with the appearance time of 12.29 min, at 213.0554 *m/z* in negative mode with two structural diagnostic ions at 169.06 and 93.03 *m/z* (Figure 9a).



**Figure 9.** MS<sup>2</sup> spectra of HBP and its degradation product obtained by LTQ-Orbitrap, (a) HBP, (b) HBP-OH.

One degradation product (called HBP-OH) at  $[\text{M} - \text{H}]^-$  229.0506  $m/z$  with an empirical formula of  $\text{C}_{13}\text{H}_{10}\text{O}_4$  was detected with an appearance time of 11.80 min (Figure 9b). Hydroxylation usually occurs during the primary degradation stage of AOPs [65]. The OH-addition on the HBP ring results in the product of HBP-OH with two main fragment ions at 211.04 and 93.03  $m/z$ .

Similar to the degradation of BP, there are also the di-hydroxylated or tri-hydroxylated products for the HBP degradation. Two di-hydroxylated products (HBP-2OH, Table 6, Figure A7) were identified at 245.0455  $m/z$  with retention times of 7.99 and 11.24 min, while one tri-hydroxylated product (HBP-3OH, Table 6, Figure A8) was found at 261.0405  $m/z$  with a retention time of 12.79 min.

The continuous attack of the ketone group by OH radicals leads to the production of compounds containing the mono-benzene ring, including benzoic acid and Pr110-b (Table 6). Benzoic acid, as the common degradation product, was also detected in the BP degradation above (Table 4) and BP3 oxidation by activate persulfate process [36]. Subsequently, the OH radical also can oxidize aromatic matter to quinone-type compounds, such as Pr152 at 151.0037  $m/z$  with the retention time of the 11.85 min (Figure A9).

Finally, OH radicals will also cleave the aromatic ring and generate small molecular compounds, such as glycolic acid, oxalic acid, malonic acid, 2-butenedioic acid, butanedioic acid, and tartronic acid (Table 7). Acetic acid and formic acid were also detected in another benzophenone-type compound BP2 degradation by photo-fenton process [43].

Therefore, a reaction pathway for the HBP degradation by the UV/ $\text{H}_2\text{O}_2$  process is also provided in Figure 10. Through hydroxylation, carboxylation, and ring cleavage, HBP is further degraded and mineralized to  $\text{CO}_2$  and water.

**Table 6.** Molecular formula and properties of HBP and its degradation products.

Code	Retention Time (min)	Molecular Formula	Theoretical $m/z$	Molecular Ions Measured $m/z$	$\Delta$ ppm	Structure
HBP	12.29	C <sub>13</sub> H <sub>10</sub> O <sub>3</sub>	213.0557	213.0556	0.47	
HBP-OH	11.80	C <sub>13</sub> H <sub>10</sub> O <sub>4</sub>	229.0506	229.0504	0.87	
HBP-2OH-a	7.99	C <sub>13</sub> H <sub>10</sub> O <sub>5</sub>	245.0455	245.0455	0.06	
HBP-2OH-b	11.24	C <sub>13</sub> H <sub>10</sub> O <sub>5</sub>	245.0455	245.0456	0.41	
HBP-3OH	12.79	C <sub>13</sub> H <sub>10</sub> O <sub>6</sub>	261.0405	261.0405	0.09	
Pr152	11.85	C <sub>7</sub> H <sub>4</sub> O <sub>4</sub>	151.0037	151.0036	0.66	
Benzoic acid	12.25	C <sub>7</sub> H <sub>6</sub> O <sub>2</sub>	121.0295	121.0296	0.82	
Pr138-b	7.38	C <sub>7</sub> H <sub>6</sub> O <sub>3</sub>	137.0244	137.0245	0.73	

**Table 7.** Degradation products of HBP detected by GC/MS.

Products	Molecular Weight	CAS Number	GC Retention Time (min)	Molecular Structure
Glycolic acid (2TMS *)	220	33581-77-0	5.43	
Oxalic acid (2TMS)	234	18294-04-7	5.33	
Malonic acid (2TMS)	248	18457-04-0	6.29	
2-Butenedioic acid (2TMS)	260	23508-82-9	6.91	
Butanedioic acid (2TMS)	262	40309-57-7	6.94	
Tartronic acid (3TMS)	336	38165-93-4	7.40	

\* TMS in the product name stands for a trimethylsilyl group.

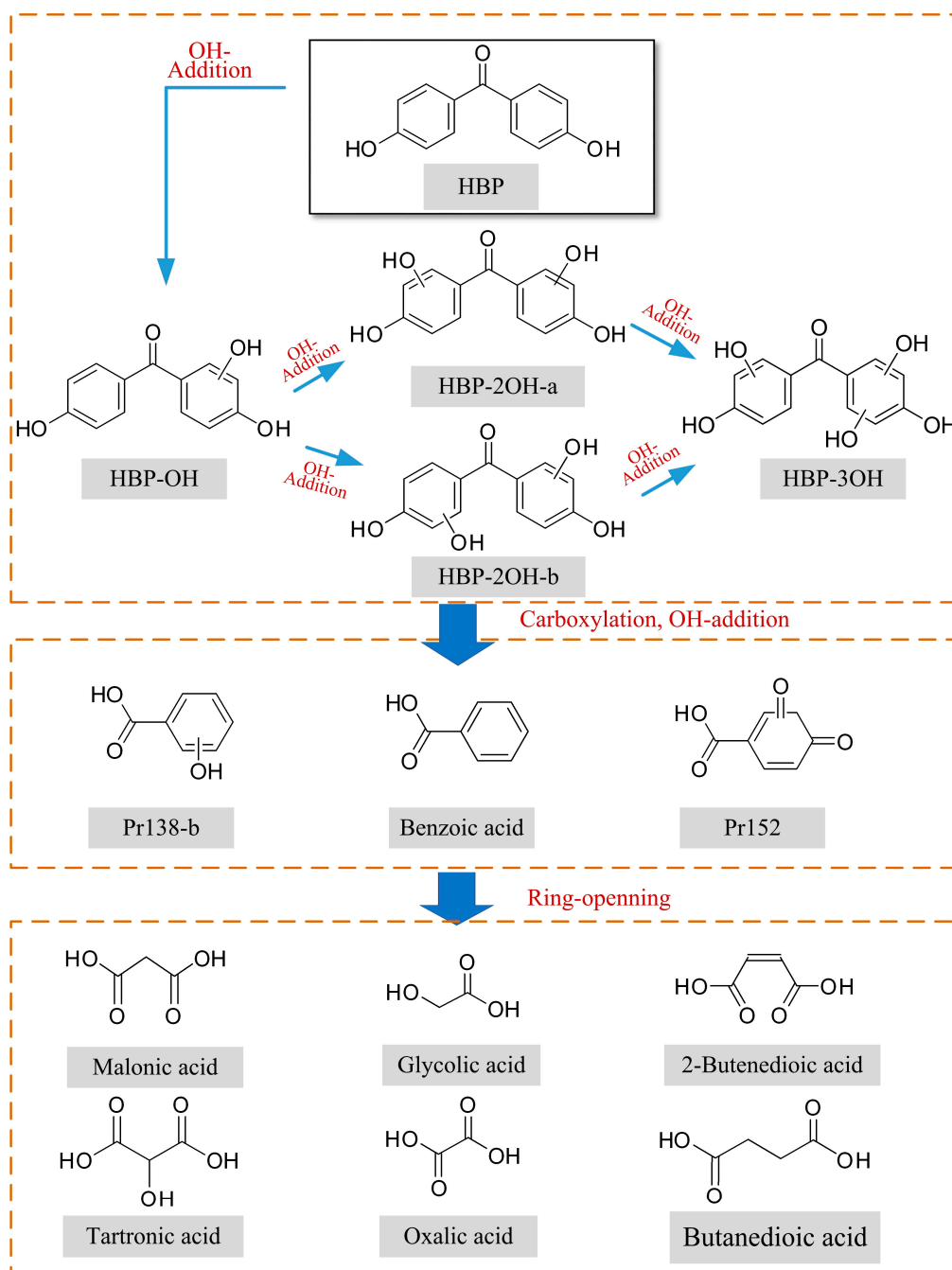


**Figure 10.** Proposed pathway of HBP degradation by the UV/H<sub>2</sub>O<sub>2</sub> process.

#### 4. Conclusions

The occurrence of benzophenone-type UV filters in wastewater and the aqueous environment has gradually drawn the attention of researchers. For the first time, two typical UV filters, BP and HBP, were selected to explore their degradation in water by a typical type of AOPs, the UV/H<sub>2</sub>O<sub>2</sub> process.

1. The built RSM model is in accordance with the experimental results and helps to elucidate the reaction factors. For both processes, the initial contaminant concentration (exerting a negative effect) were the most important factors controlling the degradation, followed by H<sub>2</sub>O<sub>2</sub> dose and UV intensity (exerting positive effects).
2. A total of 15 BP and 13 HBP degradation products were detected. There exist hydroxylated products during the BP and HBP degradation, including mono-hydroxylated, di-hydroxylated,

and tri-hydroxylated degradation products. OH radical irradiated reactions, including hydroxylation, carboxylation, and ring cleavage, result in the degradation of BP and HBP to  $\text{CO}_2$  and  $\text{H}_2\text{O}$ .

- The research provides support for the future application of UV/ $\text{H}_2\text{O}_2$  advanced oxidation processes for the treatment of wastewater containing benzophenone-type UV filters.

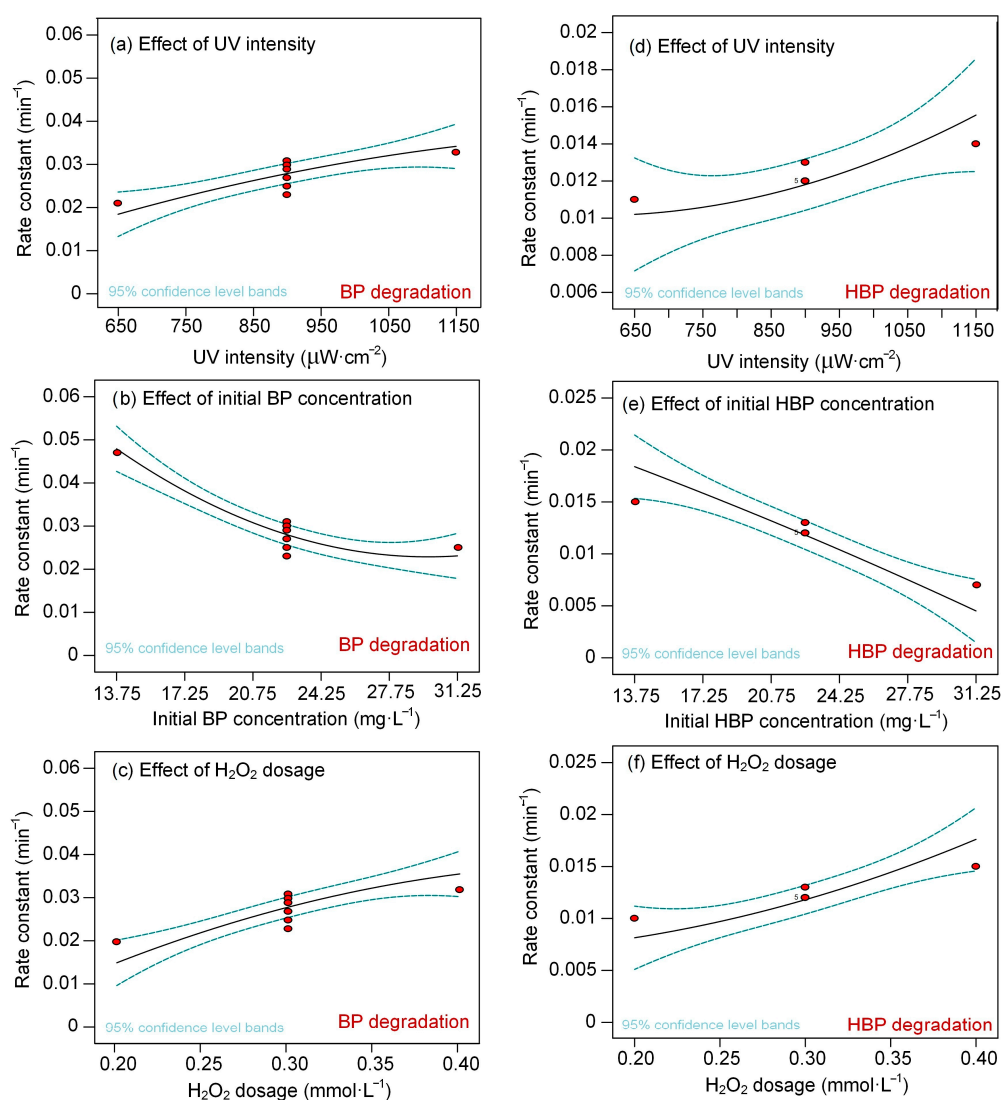
**Author Contributions:** Funding acquisition: M.L.; E.D., M.L., and X.L. conceived and designed the experiments; J.L., S.Z. and H.L. performed the experiments; E.D. analyzed the results and finished the manuscript.

**Funding:** This research was funded by the Key Special Program on the S&T for the Pollution Control and Treatment of Water Bodies (No. 2017ZX07202002); the work was also funded by Research and Practice Innovation Program for Graduate Students of Jiangsu Province (SJCX18-0960).

**Acknowledgments:** The authors would like to thank the anonymous reviewers for their valuable comments.

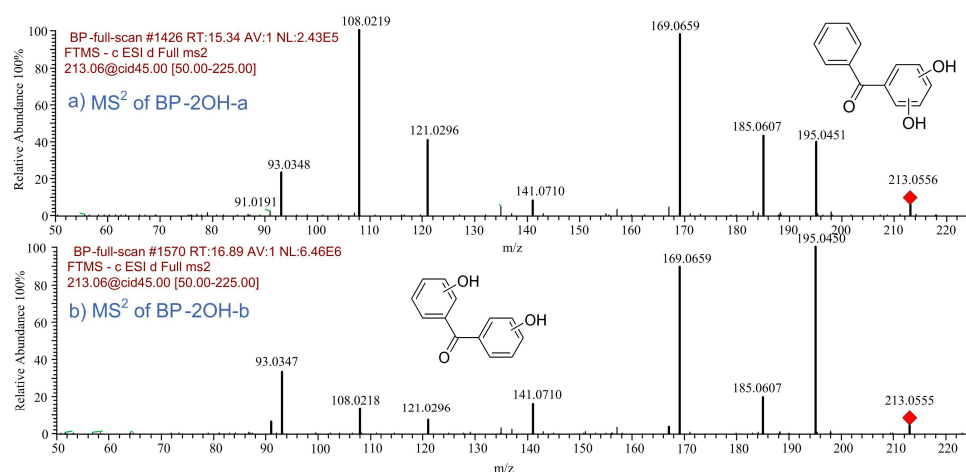
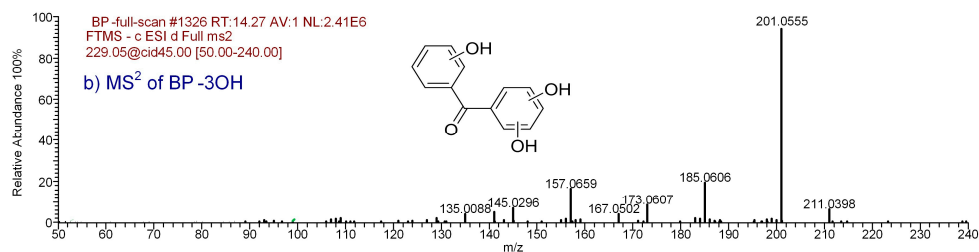
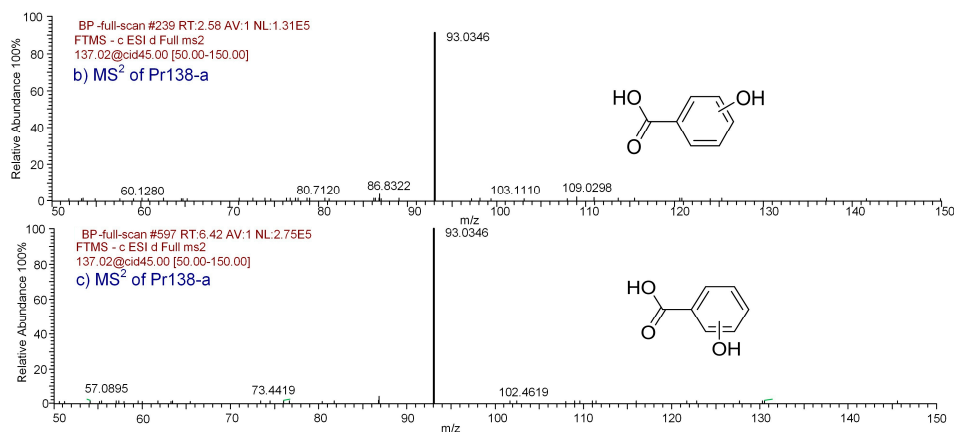
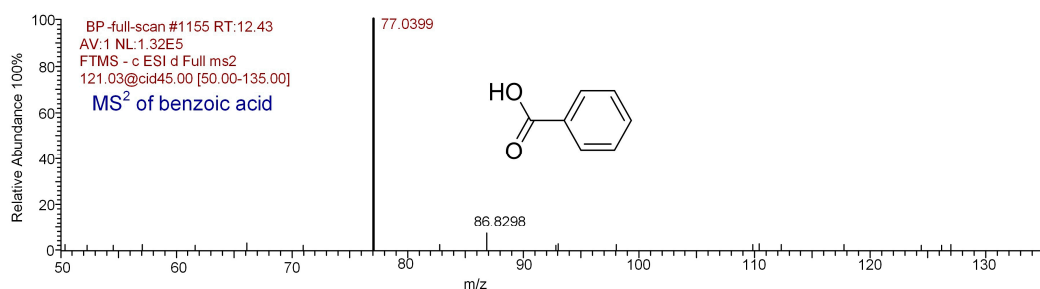
**Conflicts of Interest:** The authors declare no conflict of interest.

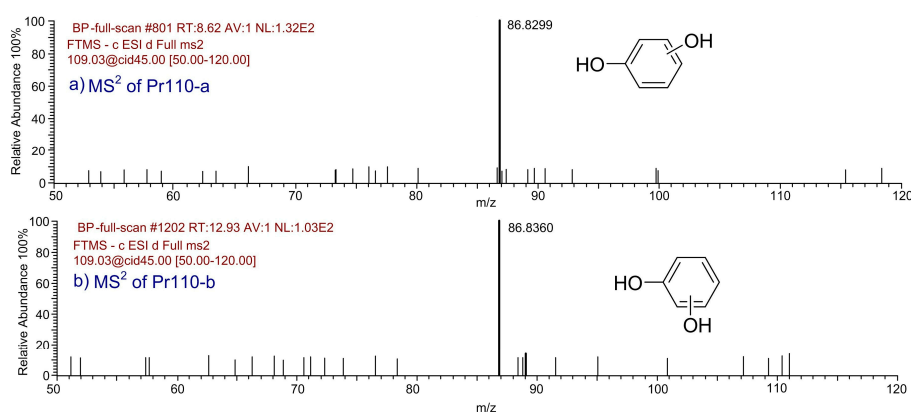
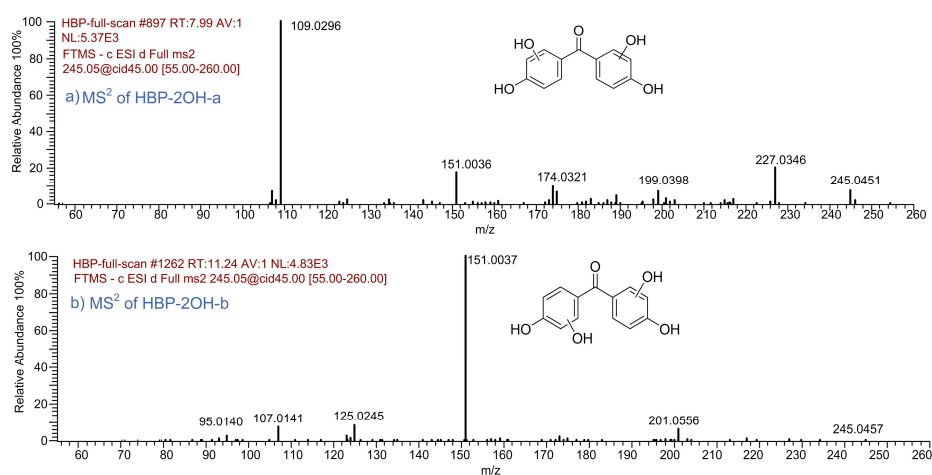
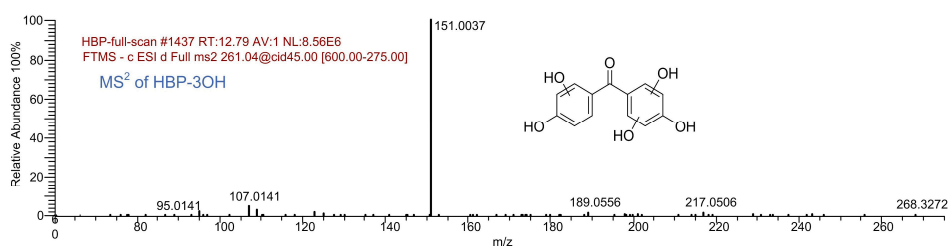
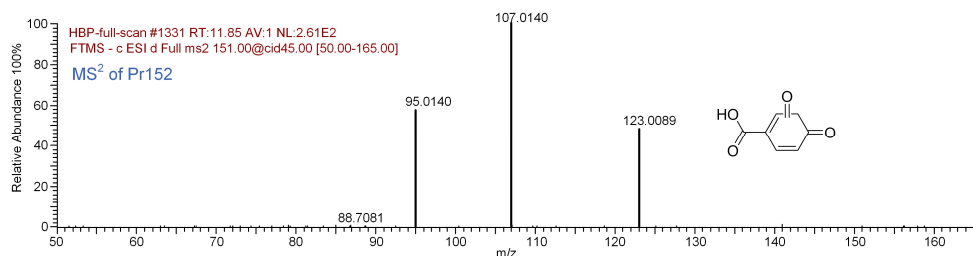
## Appendix A



**Figure A1.** The effect of single factor on the rate constants of BP and HBP degradation. (The black solid line and two blue dotted lines represent the effect of single factor and 95% confidence level bands.).



Figure A2. MS<sup>2</sup> spectra of BP-2OH-a and BP-2OH-b by HRMS.Figure A3. MS<sup>2</sup> spectra of BP-3OH by HRMS.Figure A4. MS<sup>2</sup> spectra of Pr138-a and Pr38-b by HRMS.Figure A5. MS<sup>2</sup> spectra of benzoic acid by HRMS.

Figure A6. MS<sup>2</sup> spectra of Pr110-a and Pr110-b by HRMSFigure A7. MS<sup>2</sup> spectra of HBP-2OH-a and HBP-2OH-b by HRMS.Figure A8. MS<sup>2</sup> spectra of HBP-3OH by HRMS.Figure A9. MS<sup>2</sup> spectra of Pr152 by HRMS.

## References

1. Kim, K.Y.; Ekpeghere, K.I.; Jeong, H.-J.; Oh, J.-E. Effects of the summer holiday season on UV filter and illicit drug concentrations in the Korean wastewater system and aquatic environment. *Environ. Pollut.* **2017**, *227*, 587–595. [[CrossRef](#)] [[PubMed](#)]
2. Molins-Delgado, D.; Máñez, M.; Andreu, A.; Hiraldo, F.; Eljarrat, E.; Barceló, D.; Díaz-Cruz, M.S. A potential new threat to wild life: presence of UV Filters in bird eggs from a preserved area. *Environ. Sci. Technol.* **2017**, *51*, 10983–10990. [[CrossRef](#)] [[PubMed](#)]
3. Giokas, D.L.; Salvador, A.; Chisvert, A. UV filters: From sunscreens to human body and the environment. *TrAC Trends Anal. Chem.* **2007**, *26*, 360–374. [[CrossRef](#)]
4. Chai, Q.; Zhang, S.; Wang, X.; Yang, H.; Xie, Y.F. Effect of bromide on the transformation and genotoxicity of octyl-dimethyl-p-aminobenzoic acid during chlorination. *J. Hazard. Mater.* **2017**, *324*, 626–633. [[CrossRef](#)] [[PubMed](#)]
5. Fent, K.; Zenker, A.; Rapp, M. Widespread occurrence of estrogenic UV-filters in aquatic ecosystems in Switzerland. *Environ. Pollut.* **2010**, *158*, 1817–1824. [[CrossRef](#)] [[PubMed](#)]
6. Burnett, M.E.; Wang, S. Current sunscreen controversies: A critical review. *Photodermatol. Photoimmunol. Photomed.* **2011**, *27*, 58–67. [[CrossRef](#)] [[PubMed](#)]
7. Du, Y.; Wang, W.-Q.; Pei, Z.-T.; Ahmad, F.; Xu, R.-R.; Zhang, Y.-M.; Sun, L.-W. Acute toxicity and ecological risk assessment of benzophenone-3 (BP-3) and benzophenone-4 (BP-4) in ultraviolet (UV)-filters. *Int. J. Environ. Res. Public Health* **2017**, *14*, 1414. [[CrossRef](#)] [[PubMed](#)]
8. Caliman, F.A.; Gavrilescu, M. Pharmaceuticals, personal care products and endocrine disrupting agents in the environment—a review. *CLEAN-Soil Air Water* **2009**, *37*, 277–303. [[CrossRef](#)]
9. Rodil, R.; Quintana, J.B.; Concha-Grana, E.; Lopez-Mahia, P.; Muniategui-Lorenzo, S.; Prada-Rodriguez, D. Emerging pollutants in sewage, surface and drinking water in Galicia (NW Spain). *Chemosphere* **2012**, *86*, 1040–1049. [[CrossRef](#)] [[PubMed](#)]
10. Langford, K.H.; Reid, M.J.; Fjeld, E.; Øxnevad, S.; Thomas, K.V. Environmental occurrence and risk of organic UV filters and stabilizers in multiple matrices in Norway. *Environ. Int.* **2015**, *80*, 1–7. [[CrossRef](#)] [[PubMed](#)]
11. Ramos, S.; Homem, V.; Alves, A.; Santos, L. Advances in analytical methods and occurrence of organic UV-filters in the environment—A review. *Sci. Total Environ.* **2015**, *526*, 278–311. [[CrossRef](#)] [[PubMed](#)]
12. Ekpeghere, K.I.; Kim, U.J.; O, S.H.; Kim, H.Y.; Oh, J.E. Distribution and seasonal occurrence of UV filters in rivers and wastewater treatment plants in Korea. *Sci. Total Environ.* **2016**, *542*, 121–128. [[CrossRef](#)] [[PubMed](#)]
13. Negreira, N.; Rodriguez, I.; Ramil, M.; Rubi, E.; Cela, R. Sensitive determination of salicylate and benzophenone type UV filters in water samples using solid-phase microextraction, derivatization and gas chromatography tandem mass spectrometry. *Anal. Chim. Acta.* **2009**, *638*, 36–44. [[CrossRef](#)] [[PubMed](#)]
14. Joss, A.; Siegrist, H.; Ternes, T.A. Are we about to upgrade wastewater treatment for removing organic micropollutants? *Water Sci. Technol.* **2008**, *57*, 251–255. [[CrossRef](#)] [[PubMed](#)]
15. Millh, H.; Van Eyck, K.; Dewil, R. Degradation of 4-chlorophenol by microwave-enhanced advanced oxidation processes: Kinetics and influential process parameters. *Water* **2018**, *10*, 247. [[CrossRef](#)]
16. Fang, J.; Liu, J.; Shang, C.; Fan, C. Degradation investigation of selected taste and odor compounds by a UV/Chlorine advanced oxidation process. *Int. J. Environ. Res. Public Health* **2018**, *15*, 284. [[CrossRef](#)] [[PubMed](#)]
17. Lanzafame, G.; Sarakha, M.; Fabbri, D.; Vione, D. Degradation of methyl 2-aminobenzoate (methyl anthranilate) by H<sub>2</sub>O<sub>2</sub>/UV: Effect of inorganic anions and derived radicals. *Molecules* **2017**, *22*, 619. [[CrossRef](#)] [[PubMed](#)]
18. Kudlek, E. Decomposition of contaminants of emerging concern in advanced oxidation processes. *Water* **2018**, *10*, 955. [[CrossRef](#)]
19. He, X.; Zhang, G.; de la Cruz, A.A.; O'Shea, K.E.; Dionysiou, D.D. Degradation mechanism of Cyanobacterial toxin cylindrospermopsin by hydroxyl radicals in homogeneous UV/H<sub>2</sub>O<sub>2</sub> process. *Environ. Sci. Technol.* **2014**, *48*, 4495–4504. [[CrossRef](#)] [[PubMed](#)]
20. Kim, I.Y.; Kim, M.K.; Yoon, Y.; Im, J.K.; Zoh, K.D. Kinetics and degradation mechanism of clofibric acid and diclofenac in UV photolysis and UV/H<sub>2</sub>O<sub>2</sub> reaction. *Desalin. Water Treat.* **2014**, *52*, 6211–6218. [[CrossRef](#)]
21. Jung, Y.J.; Kim, W.G.; Yoon, Y.; Kang, J.-W.; Hong, Y.M.; Kim, H.W. Removal of amoxicillin by UV and UV/H<sub>2</sub>O<sub>2</sub> processes. *Sci. Total Environ.* **2012**, *4*, 160–167. [[CrossRef](#)] [[PubMed](#)]

22. Collivignarelli, M.; Pedrazzani, R.; Sorlini, S.; Abbà, A.; Bertanza, G. H<sub>2</sub>O<sub>2</sub> based oxidation processes for the treatment of real high strength aqueous wastes. *Sustainability* **2017**, *9*, 244. [[CrossRef](#)]
23. Jang, H.-H.; Seo, G.-T.; Jeong, D.-W. Advanced oxidation processes and nanofiltration to reduce the color and chemical oxygen demand of waste soy sauce. *Sustainability* **2018**, *10*, 2929. [[CrossRef](#)]
24. Rott, E.; Kuch, B.; Lange, C.; Richter, P.; Kugele, A.; Minke, R. Removal of emerging contaminants and estrogenic activity from wastewater treatment plant effluent with UV/Chlorine and UV/H<sub>2</sub>O<sub>2</sub> advanced oxidation treatment at pilot scale. *Int. J. Environ. Res. Public Health* **2018**, *15*, 935. [[CrossRef](#)] [[PubMed](#)]
25. Gago-Ferrero, P.; Díaz-Cruz, M.S.; Barceló, D. An overview of UV-absorbing compounds (organic UV filters) in aquatic biota. *Anal. Bioanal. Chem.* **2012**, *404*, 2597–2610. [[CrossRef](#)] [[PubMed](#)]
26. Zhang, S.; Yang, X.; Chen, J.; Wei, X.; Xie, Q.; Wang, Y.; Luo, T. Aquatic environmental photochemical behavior of organic sunscreens. *Chin. Sci. Bull.* **2013**, *58*, 2989–3006. (In Chinese)
27. Lu, S.; Long, F.; Lu, P.; Lei, B.; Jiang, Z.; Liu, G.; Zhang, J.; Ma, S.; Yu, Y. Benzophenone-UV filters in personal care products and urine of schoolchildren from Shenzhen, China: Exposure assessment and possible source. *Sci. Total Environ.* **2018**, *640*, 1214–1220. [[CrossRef](#)] [[PubMed](#)]
28. Wang, L.; Kannan, K. Characteristic profiles of benzonphenone-3 and its derivatives in urine of children and adults from the United States and China. *Environ. Sci. Technol.* **2013**, *47*, 12532–12538. [[CrossRef](#)] [[PubMed](#)]
29. Kim, S.; Choi, K. Occurrences, toxicities, and ecological risks of benzophenone-3, a common component of organic sunscreen products: A mini-review. *Environ. Int.* **2014**, *70*, 143–157. [[CrossRef](#)] [[PubMed](#)]
30. Ramos, S.; Homem, V.; Alves, A.; Santos, L. A review of organic UV-filters in wastewater treatment plants. *Environ. Int.* **2016**, *86*, 24–44. [[CrossRef](#)] [[PubMed](#)]
31. Gong, P.; Yuan, H.; Zhai, P.; Xue, Y.; Li, H.; Dong, W.; Mailhot, G. Investigation on the degradation of benzophenone-3 by UV/H<sub>2</sub>O<sub>2</sub> in aqueous solution. *Chem. Eng. J.* **2015**, *277*, 97–103. [[CrossRef](#)]
32. Hopkins, Z.R.; Snowberger, S.; Blaney, L. Ozonation of the oxybenzone, octinoxate, and octocrylene UV-filters: Reaction kinetics, absorbance characteristics, and transformation products. *J. Hazard. Mater.* **2017**, *338*, 23–32. [[CrossRef](#)] [[PubMed](#)]
33. Gago-Ferrero, P.; Badia-Fabregat, M.; Olivares, A.; Piña, B.; Blánquez, P.; Vicent, T.; Caminal, G.; Díaz-Cruz, M.S.; Barceló, D. Evaluation of fungal- and photo-degradation as potential treatments for the removal of sunscreens BP3 and BP1. *Sci. Total Environ.* **2012**, *427–428*, 355–363. [[CrossRef](#)] [[PubMed](#)]
34. Duirk, S.E.; Bridenstine, D.R.; Leslie, D.C. Reaction of benzophenone UV filters in the presence of aqueous chlorine: Kinetics and chloroform formation. *Water Res.* **2013**, *47*, 579–587. [[CrossRef](#)] [[PubMed](#)]
35. Santos, A.J.M.; Miranda, M.S.; Esteves da Silva, J.C.G. The degradation products of UV filters in aqueous and chlorinated aqueous solutions. *Water Res.* **2012**, *46*, 3167–3176. [[CrossRef](#)] [[PubMed](#)]
36. Pan, X.; Yan, L.; Li, C.; Qu, R.; Wang, Z. Degradation of UV-filter benzophenone-3 in aqueous solution using persulfate catalyzed by cobalt ferrite. *Chem. Eng. J.* **2017**, *326*, 1197–1209. [[CrossRef](#)]
37. Pan, X.; Yan, L.; Qu, R.; Wang, Z. Degradation of the UV-filter benzophenone-3 in aqueous solution using persulfate activated by heat, metal ions and light. *Chemosphere* **2018**, *196*, 95–104. [[CrossRef](#)] [[PubMed](#)]
38. Liu, H.; Sun, P.; He, Q.; Feng, M.; Liu, H.; Yang, S.; Wang, L.; Wang, Z. Ozonation of the UV filter benzophenone-4 in aquatic environments: Intermediates and pathways. *Chemosphere* **2016**, *149*, 76–83. [[CrossRef](#)] [[PubMed](#)]
39. Negreira, N.; Rodríguez, I.; Rodil, R.; Cela, R. Assessment of benzophenone-4 reactivity with free chlorine by liquid chromatography quadrupole time-of-flight mass spectrometry. *Anal. Chim. Acta* **2012**, *743*, 101–110. [[CrossRef](#)] [[PubMed](#)]
40. Peng, M.; Du, E.; Li, Z.; Li, D.; Li, H. Transformation and toxicity assessment of two UV filters using UV/H<sub>2</sub>O<sub>2</sub> process. *Sci. Total Environ.* **2017**, *603*, 361–369. [[CrossRef](#)] [[PubMed](#)]
41. Ahmed, M.B.; Johir, M.A.H.; Zhou, J.L.; Ngo, H.H.; Guo, W.; Sornalingam, K. Photolytic and photocatalytic degradation of organic UV filters in contaminated water. *Curr. Opin. Green Sustain. Chem.* **2017**, *6*, 85–92. [[CrossRef](#)]
42. Murgolo, S.; Yargeau, V.; Gerbasi, R.; Visentin, F.; El Habra, N.; Ricco, G.; Lacchetti, I.; Carere, M.; Curri, M.L.; Mascolo, G. A new supported TiO<sub>2</sub> film deposited on stainless steel for the photocatalytic degradation of contaminants of emerging concern. *Chem. Eng. J.* **2017**, *318*, 103–111. [[CrossRef](#)]
43. Zúñiga-Benítez, H.; Peñuela, G.A. Application of solar photo-Fenton for benzophenone-type UV filters removal. *J. Environ. Manag.* **2018**, *217*, 929–938. [[CrossRef](#)] [[PubMed](#)]

44. Esmaili-Hafshejani, J.; Nezamzadeh-Ejhieh, A. Increased photocatalytic activity of Zn(II)/Cu(II) oxides and sulfides by coupling and supporting them onto clinoptilolite nanoparticles in the degradation of benzophenone aqueous solution. *J. Hazard. Mater.* **2016**, *316*, 194–203. [[CrossRef](#)] [[PubMed](#)]
45. Hou, Y.; Ma, J.; Sun, Z.; Yu, Y.; Zhao, L. Degradation of benzophenone in aqueous solution by Mn-Fe-K modified ceramic honeycomb-catalyzed ozonation. *J. Environ. Sci.* **2006**, *18*, 1065–1072. [[CrossRef](#)]
46. Chen, D.-Y.; Guo, X.-F.; Wang, H.; Zhang, H.-S. The natural degradation of benzophenone at low concentration in aquatic environments. *Water Sci. Technol.* **2015**, *72*, 503–509. [[CrossRef](#)] [[PubMed](#)]
47. Fujii, K.; Kikuchi, S. Degradation of Benzophenone, a Potential Xenoestrogen, by a Yeast Isolated from the Activated Sludge of a Sewage Treatment Plant in Hokkaido. *World J. Microbiol. Biotechnol.* **2005**, *21*, 1311–1315. [[CrossRef](#)]
48. Du, E.-D.; Feng, X.-X.; Guo, Y.-Q.; Peng, M.-G.; Feng, H.-Q.; Wang, J.-L.; Zhang, S. Dimethyl phthalate degradation by  $uv/h_2O_2$ : combination of experimental methods and quantum chemical calculation. *CLEAN-Soil Air Water* **2015**, *43*, 811–821. [[CrossRef](#)]
49. Ahmad, F.; Anwar, S.; Firdous, S.; Da-Chuan, Y.; Iqbal, S. Biodegradation of bispyribac sodium by a novel bacterial consortium BDAM: Optimization of degradation conditions using response surface methodology. *J. Hazard. Mater.* **2018**, *349*, 272–281. [[CrossRef](#)] [[PubMed](#)]
50. Aslani, H.; Nasser, S.; Nabizadeh, R.; Mesdaghinia, A.; Alimohammadi, M.; Nazmara, S. Haloacetic acids degradation by an efficient Ferrate/UV process: Byproduct analysis, kinetic study, and application of response surface methodology for modeling and optimization. *J. Environ. Manage.* **2017**, *203*, 218–228. [[CrossRef](#)] [[PubMed](#)]
51. Rezaee, R.; Maleki, A.; Jafari, A.; Mazloomi, S.; Zandsalimi, Y.; Mahvi, A.H. Application of response surface methodology for optimization of natural organic matter degradation by UV/ $H_2O_2$  advanced oxidation process. *J. Environ. Health. Sci.* **2014**, *12*, 67–75. [[CrossRef](#)] [[PubMed](#)]
52. Jabeen, H.; Iqbal, S.; Anwar, S.; Parales, R.E. Optimization of profenofos degradation by a novel bacterial consortium PBAC using response surface methodology. *Int. Biodeterior. Biodegrad.* **2015**, *100*, 89–97. [[CrossRef](#)]
53. Ng, K.H.; Cheng, Y.W.; Khan, M.R.; Cheng, C.K. Optimization of photocatalytic degradation of palm oil mill effluent in UV/ZnO system based on response surface methodology. *J. Environ. Manage.* **2016**, *184*, 487–493. [[CrossRef](#)] [[PubMed](#)]
54. Kasiri, M.B.; Khataee, A.R. Photooxidative decolorization of two organic dyes with different chemical structures by UV/ $H_2O_2$  process: Experimental design. *Desalination* **2011**, *270*, 151–159. [[CrossRef](#)]
55. Fu, Y.; Li, G.; Wang, R.; Zhang, F.; Qin, M. Effect of the molecular structure of acylating agents on the regioselectivity of cellulosic hydroxyl groups in ionic liquid. *Bioresources* **2016**, *12*, 992–1006. [[CrossRef](#)]
56. Li, H.; Gong, Y.; Huang, Q.; Zhang, H. Degradation of orange II by UV-assisted advanced fenton process: Response surface approach, degradation pathway, and biodegradability. *Ind. Eng. Chem. Res.* **2013**, *52*, 15560–15567. [[CrossRef](#)]
57. Peng, M.; Li, H.; Kang, X.; Du, E.; Li, D. Photo-degradation ibuprofen by UV/ $H_2O_2$  process: response surface analysis and degradation mechanism. *Water Sci. Technol.* **2017**, *75*, 2935–2951. [[CrossRef](#)] [[PubMed](#)]
58. Zuorro, A.; Fidaleo, M.; Lavecchia, R. Response surface methodology (RSM) analysis of photodegradation of sulfonated diazo dye reactive green 19 by UV/ $H_2O_2$  process. *J. Environ. Manage.* **2013**, *127*, 28–35. [[CrossRef](#)] [[PubMed](#)]
59. Rauf, M.A.; Marzouki, N.; Körbahti, B.K. Photolytic decolorization of Rose Bengal by UV/ $H_2O_2$  and data optimization using response surface method. *J. Hazard. Mater.* **2008**, *159*, 602–609. [[CrossRef](#)] [[PubMed](#)]
60. Mao, F.; He, Y.; Gin, K. Evaluating the joint toxicity of two benzophenone-type UV filters on the green alga *chlamydomonas reinhardtii* with response surface methodology. *Toxics* **2018**, *6*, 8. [[CrossRef](#)] [[PubMed](#)]
61. Jiang, Y.; Shang, Y.; Yu, S.; Liu, J. Dechlorination of hexachlorobenzene in contaminated soils using a nanometallic al/cao dispersion mixture: optimization through response surface methodology. *Int. J. Environ. Res. Public Health* **2018**, *15*, 872. [[CrossRef](#)] [[PubMed](#)]
62. Mohammadian, N.; Ghoreishi, S.; Hafeziyeh, S.; Saeidi, S.; Dionysiou, D. Optimization of synthesis conditions of carbon nanotubes via ultrasonic-assisted floating catalyst deposition using response surface methodology. *Nanomaterials* **2018**, *8*, 316. [[CrossRef](#)] [[PubMed](#)]



63. Gago-Ferrero, P.; Demeestere, K.; Silvia Díaz-Cruz, M.; Barceló, D. Ozonation and peroxone oxidation of benzophenone-3 in water: Effect of operational parameters and identification of intermediate products. *Sci. Total Environ.* **2013**, *443*, 209–217. [[CrossRef](#)] [[PubMed](#)]
64. Gago-Ferrero, P.; Díaz-Cruz, M.S.; Barceló, D. Fast pressurized liquid extraction with in-cell purification and analysis by liquid chromatography tandem mass spectrometry for the determination of UV filters and their degradation products in sediments. *Anal. Bioanal. Chem.* **2011**, *400*, 2195–2204. [[CrossRef](#)] [[PubMed](#)]
65. Li, X.; Wang, Y.; Yuan, S.; Li, Z.; Wang, B.; Huang, J.; Deng, S.; Yu, G. Degradation of the anti-inflammatory drug ibuprofen by electro-peroxone process. *Water Res.* **2014**, *63*, 81–93. [[CrossRef](#)] [[PubMed](#)]



© 2018 by the authors. Licensee MDPI, Basel, Switzerland. This article is an open access article distributed under the terms and conditions of the Creative Commons Attribution (CC BY) license (<http://creativecommons.org/licenses/by/4.0/>).